Drug Delivery and Translational Research
https://doi.org/10.1007/s13346-022-01166-x

ORIGINAL ARTICLE

Preclinical efficacy and safety of novel SNAT against SARS-CoV-2 using a hamster model

Lok R. Pokhrel[1] · Frank Williams[2] · Paul P. Cook[3] · Dorcas O'Rourke[4] · Gina Murray[5] · Shaw M. Akula[2]

Accepted: 7 April 2022

Abstract

To address the unprecedented global public health crisis due to severe acute respiratory syndrome coronavirus 2 (SARS-CoV-2), we designed and developed a novel antiviral nano-drug, called SNAT (Smart Nano-Enabled Antiviral Therapeutic), comprised of taxoid (Tx)-decorated amino (NH_2)-functionalized near-atomic size positively charged silver nanoparticles (Tx–[NH_2-AgNPs]) that are stable for over 3 years. Using a hamster model, we tested the preclinical efficacy of inhaled SNAT on the body weight, virus titer, and histopathology of lungs in SARS-CoV-2-infected hamsters, including biocompatibility in human lung epithelium and dermal fibroblasts using lactase dehydrogenase (LDH) and malondialdehyde (MDA) assays. Our results showed SNAT could effectively reverse the body weight loss, reduce the virus load in oral swabs, and improve lung health in hamsters. Furthermore, LDH assay showed SNAT is noncytotoxic, and MDA assay demonstrated SNAT to be an antioxidant, potentially quenching lipid peroxidation, in both the human cells. Overall, these promising pilot preclinical findings suggest SNAT as a novel, safer antiviral drug lead against SARS-CoV-2 infection and may find applications as a platform technology against other respiratory viruses of epidemic and pandemic potential.

Keywords Antiviral drug candidate · SARS-CoV-2 · COVID-19 · SNAT · Inhaler · Nanotechnology

Background

COVID-19 (Corona virus Disease 2019) is an ongoing pandemic caused by severe acute respiratory syndrome coronavirus 2 (SARS-CoV-2) [1]. SARS-CoV-2 is more transmissible and infectious than any other corona/influenza viruses, primarily affecting human respiratory system with secondary infections leading to sepsis, organ damage, and ultimately death [2]. SARS-CoV-2 infection causes mild to severe respiratory pneumonia, with symptoms appearing 2–10 days post-infection [3], followed by extrapulmonary

Highlights
1. SNAT was designed, developed, and tested for preclinical efficacy against SARS-CoV-2.
2. Inhaled SNAT could significantly protect hamster from body weight loss.
3. SNAT could significantly reduce virus load and improve lung health in hamster.
4. SNAT is noncytotoxic and acted as antioxidant in human lung and skin cells.
5. SNAT may serve as a potent, safer antiviral nano-drug lead against SARS-CoV-2.

✉ Lok R. Pokhrel
pokhrell18@ecu.edu

✉ Shaw M. Akula
akulas@ecu.edu

[1] Department of Public Health, The Brody School of Medicine, East Carolina University, Greenville, NC 27834, USA

[2] Department of Microbiology and Immunology, The Brody School of Medicine, East Carolina University, Greenville, NC 27834, USA

[3] Department of Internal Medicine, The Brody School of Medicine, East Carolina University, Greenville, NC 27834, USA

[4] Department of Comparative Medicine, The Brody School of Medicine, East Carolina University, Greenville, NC 27834, USA

[5] Department of Pathology & Laboratory Medicine, The Brody School of Medicine, East Carolina University, Greenville, NC 27834, USA

Published online: 19 April 2022

manifestations in about 10% of patients causing multiorgan failure including the lungs, kidneys, heart, and liver [1, 2]. Bacterial and fungal infections are common in COVID-19 patients that often succumb to the disease [4–6].

Currently, vaccines are being used to successfully thwart COVID-19 around the world. The major limitation of current vaccines is the emergence of multiple viral variants with potentially increased pathogenicity and ability to infect younger children, the breakthrough infections as observed in those vaccinated, and patients suffering from "Long Covid"—a diverse set of debilitating symptoms that persists for several months [4, 5]. Among the variety of drugs that have been tested against COVID-19, FDA recently approved Remdesivir and dexamethasone [6]; but these have their own limitations and are effective only when administered very early during the infectious cycle. Hence, there is an urgency to address the unmet need for innovative technologies and platforms that can lead to novel therapeutics and preventive solutions with potential to neutralize SARS-CoV-2 and halt COVID-19 progression and death.

Nanotechnology allows for smart designing of therapeutics and/or vaccines affording broad-spectrum mode of actions, unlike single organic compound-based drugs often created via conventional (organic) synthesis methods. Previously, chitosan-based nanospheres containing acyclovir (average size 200 nm) demonstrated higher efficacy against HSV-1 and HSV-2 compared to acyclovir alone in an in vitro skin permeation assay [7]. Likewise, vitamin-E-based nanoparticulates encapsulating adenosine and squalene were found to mitigate hyperinflammation by reducing TNF-a in SARS-CoV-2-infected mice [8]. Utilizing nanotechnology platform, Novavax developed spike (S) protein-based nanovaccine against COVID-19 [9]. As for diagnostics, nanogold has been used by World Nano Foundation to develop rapid IgM/IgG antibody assay kit for testing SARS-CoV-2 infections [10]. Additional details on other types of nanoformulations being developed by researchers around the world to address virus infections can be found in the review by Chakravarty and Vora [11].

Given the increasing prospects that nanotechnology hold in thwarting the COVID-19 pandemic, in this project, we tested the anti-SARS-CoV-2 properties of the Smart Nano-enabled Combination Antiviral Therapy (SNAT) using a hamster model. SNAT comprises of a near atomic size and highly positively charged "seed" of amino-functionalized silver nanoparticles (NH_2-AgNPs) surface decorated with a low-concentration (1 μg/mL) of a taxoid antineoplastic agent, docetaxel (Tx). Several key features of SNAT motivated us to explore it as a potential therapeutic agent against SARS-CoV-2: (i) its broad spectrum antibacterial and antifungal activities that could inhibit secondary infections in COVID-19 patients [12, 13]; (ii) Tx improves bioavailability and solubility/stability of the NPs and may improve the outcome in lung cancer patients with COVID-19; and (iii) an alkaline pH of SNAT (pH 7.5–8.5) could block endosomal viral release at pH ≥ 7, potentially interfering with the virus lifecycle [14]. Accordingly, we hypothesized SNAT to alleviate SARS-CoV-2-induced body weight loss, reduce virus load, and protect lung health in hamsters. We used golden Syrian hamsters in this study as it is a widely used experimental animal model and has previously been reported to support replication of SARS-CoV-2 [15, 16]. SARS-CoV-2 infection in golden hamsters resembles those found in humans and the pathology is pronounced in the respiratory tract, and disease signs and endpoints include weight loss and presence of infectious virus in nostrils and lungs [17]. Our data demonstrate the ability of SNAT to not only reverse the effects of SARS-CoV-2 infection on the body weight loss but also significantly lower virus titer in the oropharyngeal cavity (i.e., oral swab).

Methods

Cells

Vero cells and dermal fibroblast (106-05A-1526; Millipore Sigma) cells were used in this study. The cells were cultured in Dulbecco's modified Eagle medium (DMEM) (Invitrogen, Carlsbad, CA) containing 10% charcoal-stripped fetal bovine serum, L-glutamine, and antibiotics as per earlier standard protocols [18]. We also used human lung epithelial (H-6053; Cell Biologics) cells that were cultured in complete medium recommended by the manufacturer as per standard protocols. Vero cells were used for infection assays while the human lung epithelial and dermal fibroblast cells were used for LDH and MDA assays.

Virus

All work pertaining to the use of SARS-CoV-2 were performed in BSL-3 laboratory. SARS-CoV-2 (isolate USA-WA1/2020) purchased from bei RESOURCES (Manassas, VA) was propagated in Vero cells as per standard procedures [19]. SARS-CoV-2 virus was propagated in Vero cells, purified and concentrated using 10–30% sucrose gradient in an ultracentrifuge (Beckman L8-55), and the yield titrated as per standard protocols [20]. The following research was approved by the Office of Prospective Health/Biological Safety for the use of biohazardous agent (SARS-CoV-2) and the registration number is 20–01 (title: Host response to COVID-19 infection in Eastern North Carolina).

SNAT synthesis and characterization

SNAT (Tx–[NH_2-AgNPs]; US Patent No. 63/042,070) was synthesized in-house using the "seed" of our patented

NH_2-AgNPs (US Patent No. PCT/US2021/014343). The synthesis followed one-pot design using $UV_{254\ nm}$ irradiation for 6 h followed by heating at 95 °C for 45 min, then KBH_4 reduction, and cooling at room temperature overnight, followed by Docetaxel addition and warming at 60 °C with gentle stirring for 12 h. SNAT thus synthesized was purified using 3.5 kD dialysis membranes (Spectra/Por 3.5kD dialysis kit). Purified SNAT was characterized in detail using multiple complementary techniques: electron microscopy (TEM, Philips EM 420), energy dispersive spectroscopy (EDS), dynamic light scattering (DLS; Malvern Zetasizer Nano ZS90), UV–Vis spectrophotometer (Hach DR6000), and other physicochemical analyses (pH, electrical conductance).

Potential stability of SNAT and seed NH_2-AgNPs were also measured as a function of time (0–3 years), incubating at room temperature (25 °C), using DLS and UV–Vis spectrophotometer.

SNAT administration

Each hamster was exposed to two doses of 10 µg/mL SNAT (2 mL/dose) in a modified nose-only inhalation exposure equipment. Briefly, the nebulizer (UNOSEK nebulizer) was connected to the modified SCIREQ nose only exposure chamber that was conveniently fit inside the BSL-3 biosafety cabinet. The key features of the nebulizer are as follows: atomization rate: ≥ 0.2 mL/min; aerosol size range: 0.5–5 µm; mean aerosol diameter: 2.81 ± 0.14 µm; and drug delivery rate: 75.7%; capacity: 8 mL max, 0.2 mL/min. This nebulizer uses the compressed air technology that allows for high nebulization rate.

LDH cytotoxicity assay

The lactate dehydrogenase (LDH) assay was performed using the CytoTox 96 non-radioactive kit (Promega) as per earlier studies [21]. Target cells (human lung epithelial and dermal fibroblast cells) were treated with different concentrations of SNAT at 37 °C in a V-bottom 96-well plate. After 24 h incubation, the cells were analyzed for the expression of LDH, as an indicator of cell death. G418 at 1 mg/mL concentration (Sigma-Aldrich, St. Louis, MO) was used as a known cell death inducer.

MDA assay

We tested potential lipid peroxidation (malondialdehyde [MDA] assay) in human lung epithelial and dermal fibroblast cells upon SNAT treatments (0.05–10 µg/mL) to assess its biocompatibility with human cells in vitro as per standard manufacturer's protocol (Abcam; ab118970) [22]. Cells were cultured in DMEM containing 10% charcoal-stripped fetal bovine serum, L-glutamine, and antibiotics in round bottom 96 well plates. The samples were quantified colorimetrically using a microplate reader at 532 nm. Each reaction was done in triplicate. Sterile water (dilution buffer) was used as a negative control and hydrogen peroxide (200 µM) was used as a positive control.

Hamster infection experiment

Our Animal Use Protocol entitled, "Effect of SNAT on SARS-CoV-2 infection of hamsters" (AUP #K177) was reviewed by ECU Institution's Animal Care and Use Committee (approval date: 11/12/2020). The study involved four groups ($n = 8$ per group) of male Syrian hamsters (*Mesocricetus auratus*) aged 6–8 weeks and procured from Jackson Laboratory. The four groups were (i) uninfected; (ii) SARS-CoV-2 infected; (iii) SARS-CoV-2 infected and saline administered; and (iv) SARS-CoV-2 infected and SNAT administered following 2 h of virus inoculation (on day 1) and second dose on day 2. A simplified schematic showing the study design is depicted in Fig. 1. The animals were anesthetized by inhalation of vaporized isoflurane using an IMPAC6 veterinary anesthesia machine for the following procedures: intranasal challenge of virus, recoding body weight, obtaining oral swabs, and for euthanizing animals.

Viral RNA quantitation

The oral swabs were collected and stored in 1 mL UTM transport media (Copan, Murrieta, CA). The media was used to obtain RNA from the specimens as per standard laboratory procedures using QIAmp viral RNA kits (Qiagen, Georgetown, MD). The RNA concentrations were measured with a NanoDrop ND-2000 spectrophotometer (Thermo Fisher Scientific, Waltham, MA, USA). The viral copy numbers in the extracted RNA were determined by RT-qPCR using the 2019-nCoV RUO kit as per the manufacturer protocols (Integrated DNA technologies, Coralville, IA).

Preparation of lung tissues for histology

Lung tissues collected on day 3 post-infection were fixed in 10% neutral buffered formalin, trimmed, processed, embedded in paraffin, cut at 5 to 6 µm, and stained with hematoxylin and eosin (H&E).

Statistical analysis

Univariate analysis of variance (ANOVA) was used to compare between the treatment means and the controls, and the data satisfied normal probability distribution. Data were visualized using scatter or bar plots. Statistical significance

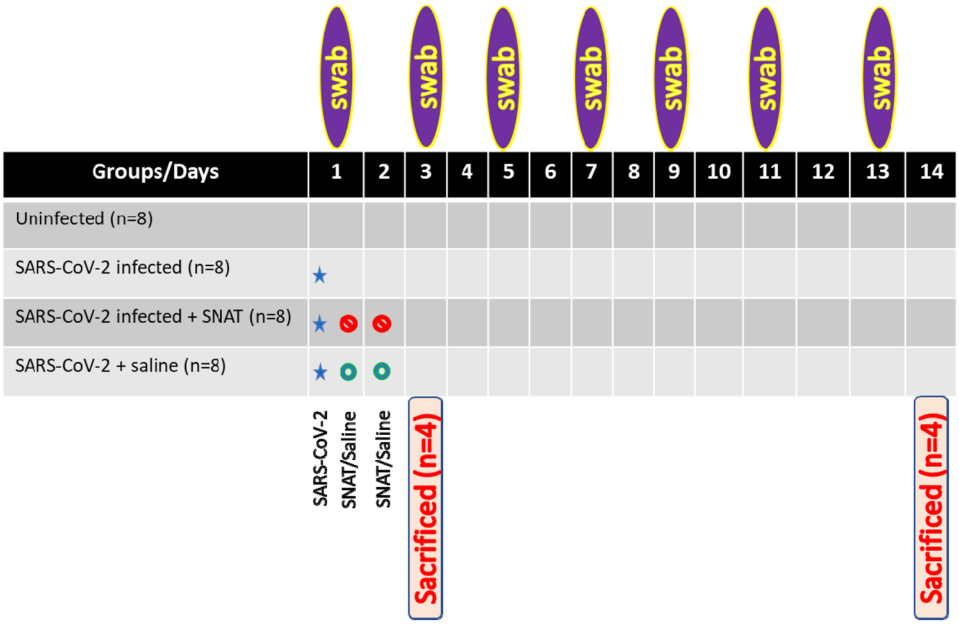

Fig. 1 A schematic depicting the study design used for testing the efficacy of SNAT on SARS-CoV-2-infected golden Syrian hamsters

was established at 0.05 level. All data were analyzed using IBM SPSS 26.0 (Armonk, NY: IBM Corp.).

Results and discussion

SNAT characterization

The amino-functionalized silver nanoparticles (NH_2-AgNPs) had a mean TEM diameter of 5.8 nm ± 2.8 nm (S.D.) with a spherical morphology and the core composed of elemental/metallic silver (Ag^0) surface functionalized with cationic NH_2-functional group (Fig. 2A, B). Upon surface decorating with docetaxel (Tx) led to the formation of Tx–[NH_2-AgNPs], i.e., SNAT, whereby two or more individual NH_2-AgNPs (blue arrow) self-assembled presenting a near triangular architecture collectively embedded within Tx molecules (red arrow; Fig. 2C). The average hydrodynamic diameters (HDDs) for NH_2-AgNPs and SNAT were similar: 4.3 nm and 5.0 nm, respectively, suggesting that Tx binding did not influence the original TEM particle size of seed NH_2-AgNPs. Both the NH_2-AgNPs and SNAT had high positive mean surface zeta potentials: + 41 mV and + 22 mV, respectively, and are highly stable for over 3 years at room temperature (25 °C) as the standard deviation for HDD was within ± 1 nm and within ± 3 mV for zeta potential over the 3-year period (Supplementary Table S1). Furthermore, no change in λ_{max} over the 3-year period confirmed these DLS results (Supplementary Table S1). Thus, these stability data suggest there is no need for refrigeration during transportation and storage and may serve as an ideal antiviral agent for low resource settings where cold storage chain is unavailable. The blue-shift of 40 nm and red-shift of 14 nm as demonstrated by the UV–Vis spectra suggest a strong electrostatic binding of anionic Tx with cationic NH_2-groups on the surface of AgNPs (Fig. 2D). The representative EDS spectra and elemental composition (mass/atom %) for SNAT are presented in Fig. 2E, F, showing that SNAT was composed of Ag, C, O, and N. The dialysis-purified SNAT and NH_2-AgNP formulations had an alkaline pH (7.5–8.5) and low electrical conductance of 0.120 mS/cm.

Determining the optimal dose of SNAT for hamster studies

The optimal dose of SNAT to be used in animal studies was determined testing SNAT in physiologically relevant cells. We tested different doses of SNAT in human lung epithelial cells using an LDH assay. SNAT doses equal to or below 10 µg/mL did not induce any significant cell death (Fig. 3A). Understanding virus-induced oxidative stress is pivotal in the viral life cycle including the pathogenesis of ensuing disease. Reactive oxygen species (ROS) are generated upon virus infection, and in response, a host cell activates an anti-oxidative defense system for protection [22, 23]. Understanding potential interaction between a virus and a host is critical to developing antivirals that could control viral infection. Many viruses, including SARS-CoV-2, are known to induce oxidative stress to facilitate their replication inside the host

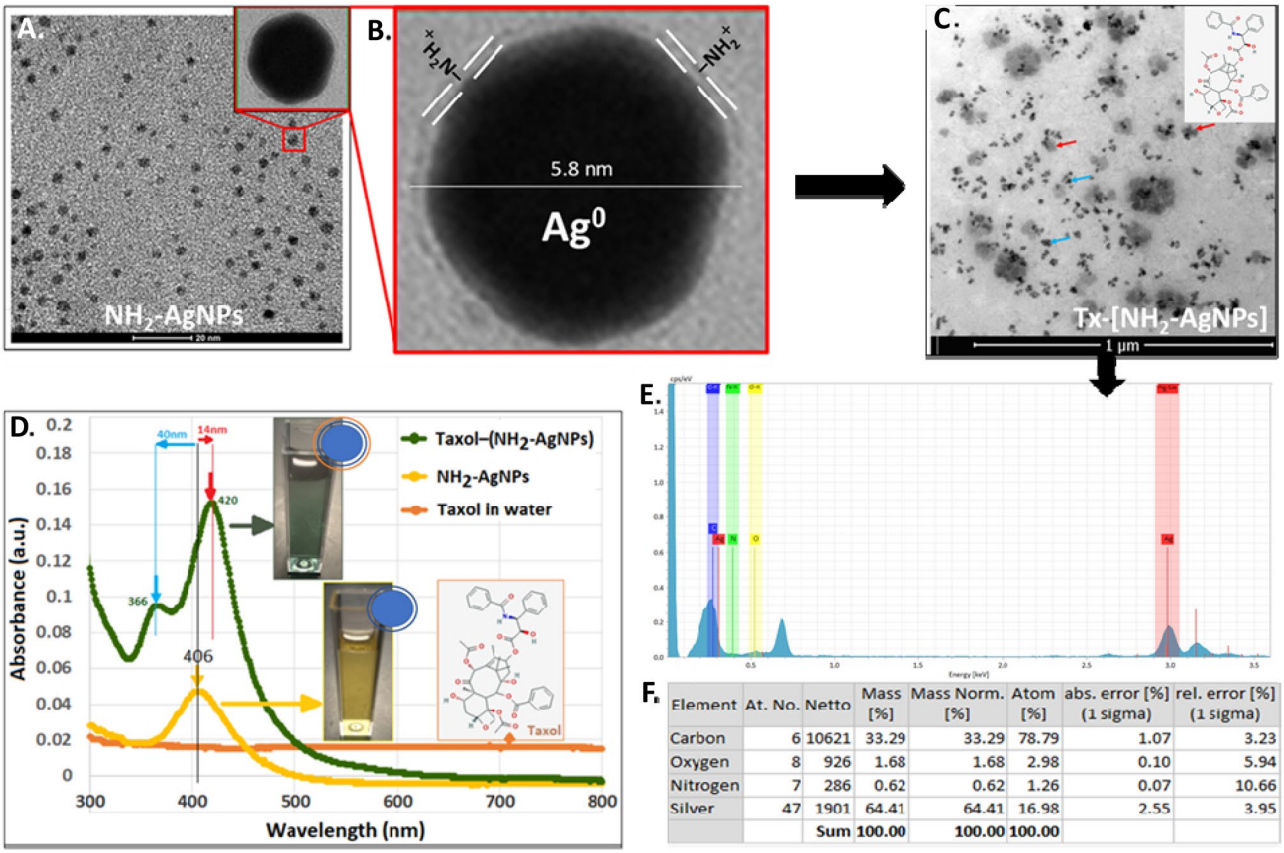

Element	At. No.	Netto	Mass [%]	Mass Norm. [%]	Atom [%]	abs. error [%] (1 sigma)	rel. error [%] (1 sigma)
Carbon	6	10621	33.29	33.29	78.79	1.07	3.23
Oxygen	8	926	1.68	1.68	2.98	0.10	5.94
Nitrogen	7	286	0.62	0.62	1.26	0.07	10.66
Silver	47	1901	64.41	64.41	16.98	2.55	3.95
		Sum	100.00	100.00	100.00		

Fig. 2 Detail characterization of SNAT. Representative high resolution-transmission electron microscopy (HR-TEM) image of the "seed" amino-functionalized silver nanoparticles (NH_2-AgNPs) showing spherical particle morphology of elemental/metallic silver (Ag^0) with mean particle diameter of 5.8 nm ± 2.8 nm **A** and **B**. S/TEM micrographs of SNAT: surface docetaxel (Tx)-decorated (red arrow) amino-functionalized silver nanoparticles (Tx–[NH_2-AgNPs]) showing two or more individual NH_2-AgNPs (blue arrow), each ~ 5 nm diameter, self-assembled forming a somewhat triangular architecture collectively embedded within Tx molecules **C**. Inset in C shows the molecular structure of Tx. UV–Vis spectra of docetaxel (Tx)-decorated amino-functionalized silver nanoparticles (Tx–[NH_2-AgNPs]) (green spectrum/red arrow; (blue) green suspension), NH_2-AgNPs alone (yellow spectrum, yellow suspension), and Tx alone (in sterile Milli-Q water) (orange spectrum showing a flat line; inset to the right showing molecular structure of Tx) **D**. The "seed" of NH_2-AgNPs alone had a maximum absorbance (λ_{max}) at 406 nm, which red-shifted to 420 nm (a change of 14 nm) and blue shifted to 366 nm (a change of 40 nm) upon direct surface binding with Tx molecules. Representative EDS spectra and elemental composition (mass/atom %) of SNAT **E** and **F**

[24–26]. Lipid peroxidation occurs when excess ROS affects cell membranes and can also lead to oxidation and denaturation of proteins and DNA damage, further inducing inflammatory immune responses and cell death [27]. Our results show no lipid peroxidation (MDA) in human lung epithelial and dermal fibroblast cells upon SNAT treatments as the MDA levels were all below the background concentrations (negative control, dilution buffer). Rather, data revealed a decrease in MDA with up to 10 µg/mL of SNAT treatments in lung cells compared to treatments with the negative control (dilution buffer) or the positive control (hydrogen peroxide) (Fig. 3B, C). Such an ability to quench oxidative stress response makes SNAT an exciting antiviral candidate.

We also performed in vitro neutralization studies against SARS-CoV-2 to determine if Tx alone, NH_2-AgNPs alone, and SNAT would neutralize the virus. We found that Tx (1 µg/mL) or NH_2-AgNPs (10 µg/mL) alone did not neutralize the virus in vitro, but SNAT (10 µg/mL) did (data not shown). This led us to choose SNAT, over Tx (1 µg/mL) or NH_2-AgNPs (10 µg/mL) alone, for the detailed hamster studies.

Based on the above in vitro neutralization effects of SNAT, we further tested doses of 1 µg/mL, 5 µg/mL, and 10 µg/mL of SNAT (2 mL/dose) administered using a nose-only inhalation exposure equipment to hamsters ($n = 2$/group). The animals were administered SNAT on day 1 and day 2 (24 h after the first dose). The animals were monitored for any signs of distress and body weight. All animals survived the 12-day screening period. There was no significant body weight loss in the animals that received 1, 5, or 10 µg/mL of SNAT (data not shown). Therefore, we decided to use 10 µg/mL of SNAT in the challenge studies.

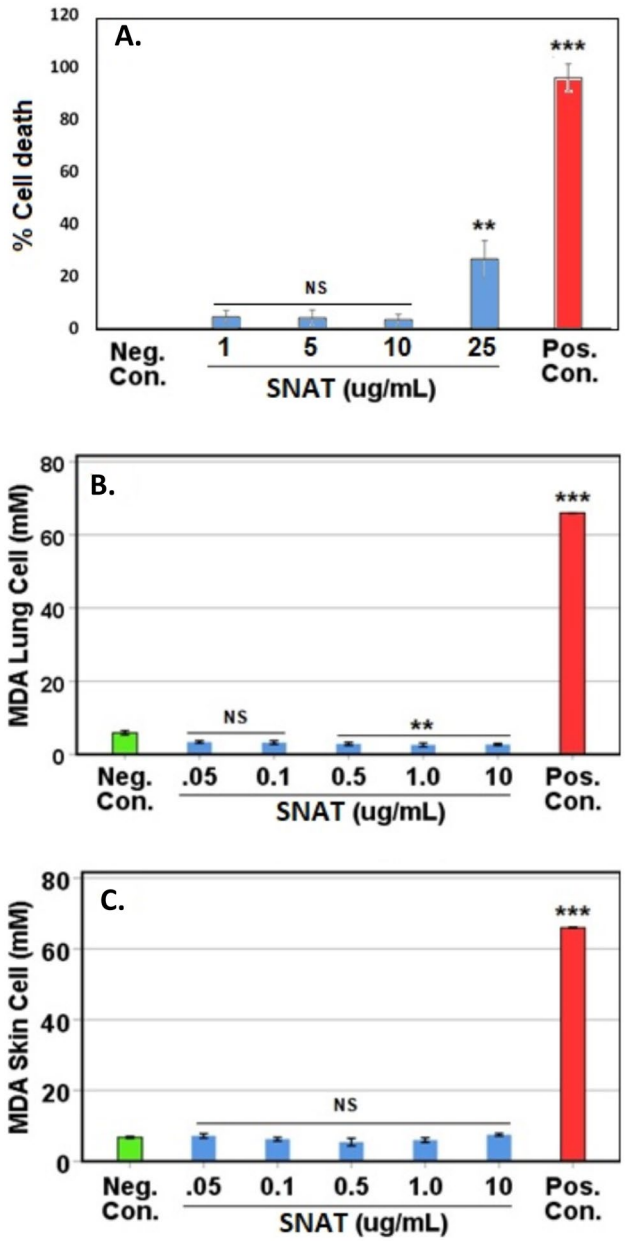

Fig. 3 SNAT is safer to human cells. To determine the cytotoxic effect of SNAT on human lung epithelial and dermal fibroblast cells, at 24 h post SNAT treatment, lactate dehydrogenase (LDH) release as an indicator of percentage of cell death was monitored. Known inducer of cell death, 1 mg/mL G418, was used as a positive control in this study **A**. Effect of SNAT on oxidative stress. In vitro oxidative stress response assessment of SNAT in primary human lung epithelial cells **B** and dermal fibroblast cells **C**, showing no malondialdehyde (MDA) lipid peroxidation in both the cell assays. Average of three experiments is depicted in the plot. "**" denotes significantly lower compared to negative control ($p < 0.05$); "***" denotes significantly higher compared to negative control ($p < 0.001$); and NS denotes each treatment group is not significantly different from negative control ($p > 0.05$). Negative control denotes diluent buffer (sterile water), and positive control denotes hydrogen peroxide (200 µM)

SNAT reduces SARS-CoV-2 load in hamsters

In COVID-19 patients with acute respiratory illness, the main clinical manifestation is severe lung inflammation [28]. Since SARS-CoV-2 induces severe pathological lesions in the lungs of these Syrian hamsters, we chose to use this animal model [16]. As a direct measure of SARS-CoV-2 infection of hamsters, we monitored virus titer in the oral swabs collected from hamsters on day 01 and every other day post infection. The effect of SNAT inhalation on virus infection of hamsters was monitored by performing virus titration in Vero cells to calculate $TCID_{50}$ and by determining viral RNA copy numbers using RT-qPCR. Our study demonstrated SNAT to significantly lower virus infection in oral swabs by day 05 as observed by $TCID_{50}$ (Fig. 4A) and a sharp decline in the viral RNA copy numbers (Fig. 4B). There was a significant decrease in viral titers in oral swabs taken from SARS-CoV-2 infected hamsters exposed to SNAT compared to those that were SARS-CoV-2 infected or those infected but received saline (Fig. 4A). The levels of virus titer reduction (one log or ten-fold) were substantial in animals that were treated with SNAT compared to saline or untreated group (Fig. 4A).

SNAT protects SARS-CoV-2-infected hamsters from body weight loss

SARS-CoV-2 infection of hamsters resulted in a significant body weight loss by 3 days post infection when compared to uninfected hamsters (Fig. 5). The body weight loss in virus infected hamsters was the greatest during the first week of infection. As a result of viral load reductions in hamsters and improved lung health, hamsters that received SNAT could alleviate the virus-induced body weight loss to a significant extent compared to the group that received saline (Fig. 5). Taken together, the results of this study demonstrate the potential of SNAT to significantly lower SARS-CoV-2 infection and the ensuing lung pathology. Future studies are aimed at deciphering the mechanism by which SNAT inhibits SARS-CoV-2 infection in hamsters.

SNAT ameliorates lung injury in SARS-CoV-2-infected hamsters

We further examined the early histopathological changes in the lungs of hamsters to understand the effects of SARS-CoV-2 and SNAT treatment (Fig. 6). SARS-CoV-2 infection induced significant changes in lungs (Fig. 6; panels 2.0 and 2.1) compared to lungs from uninfected hamsters at 3 dPI (Fig. 6; panels 1.0 and 1.1). SARS-CoV-2 infection induced

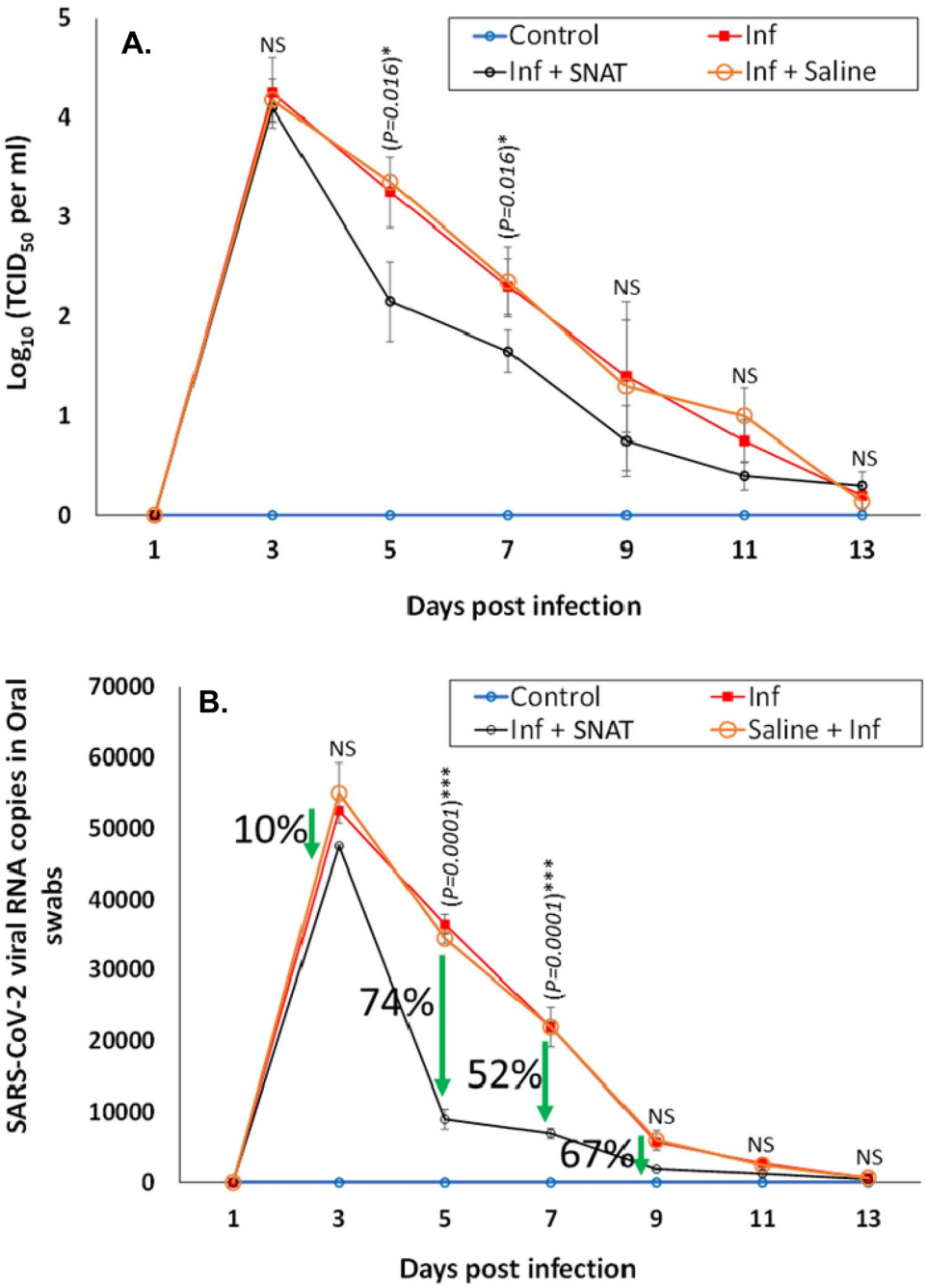

Fig. 4 SNAT treatment significantly lowers SARS-CoV-2 titers in the oral secretions. Oral swab suspension collected on different days were tested for virus yield in Vero cells and the $TCID_{50}$ was calculated using the Reed and Muench formula as per standard protocols. RNA was extracted from 140 µL of oral swab suspension using QIAmp viral RNA extraction kit (Qiagen) as per standard protocols. The RNA concentrations were measured with a NanoDrop ND-2000 spectrophotometer (Thermo Fisher Scientific, Waltham, MA, USA). The virus concentration in the specimens were detected by qPCR monitoring nucleocapsid N gene using the SARS-CoV-2 (2019-nCoV) CDC qPCR Probe Assay (Integrated DNA technologies). The limit of detection for this assay is 50 copies. For panels **A** and **B**, each point represents mean ± S.D. of three individual experiments. ANOVA was used to compare between group means. Between groups differences are significant at $p < 0.05$, denoted by *; day 5 through day 13 were significantly different at $p < 0.01$, denoted by **

patchy evidence of oedema, hemorrhage and vascular congestion, subtle mononuclear infiltration, and focal hyaline membrane formation. The lungs of SARS-CoV-2 infected hamsters that received inhaled SNAT showed significantly lower signs of lung injury with no focal hyaline membrane formation (Fig. 6; panels 3.0 and 3.1), suggesting SNAT's potential to effectively reduce the lung injury from SARS-CoV-2 infection.

Nano-based therapeutics are considered an adaptable alternative to conventional small molecules such as antibodies for the neutralization of viruses. Because variable linkers can be decorated on to the surface of the nanoparticles, multivalent interactions of such nanoparticle drug candidates can be expected with the virus surfaces, potentially leading to virus neutralization [29, 30]. Such approach has been previously described to combat various RNA virus infections like HIV, paramyxovirus, SARS-CoV-2, and others [31–33]. The surface-modified multivalent SNAT that we developed has strong potential application as an inhalation antiviral therapeutic while conferring adequate safety to the lung and skin cells [29, 30].

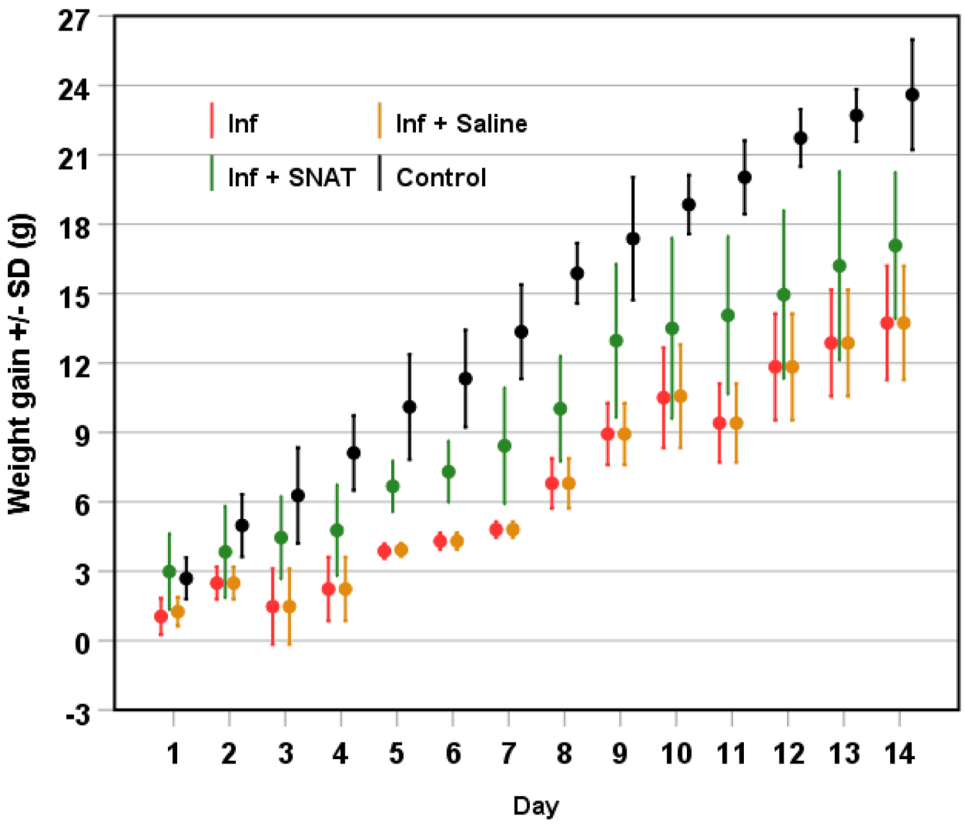

Fig. 5 SNAT treatment protects SARS-CoV-2-infected hamsters from body weight loss. SNAT treatment significantly protects SARS-CoV-2-infected hamsters from weight loss. Although weight loss began day 1 post infection (PI), the highest weight loss occurred during the first week of infection for the SARS-CoV-2-infected group compared to the control-uninfected group. Percent weight loss was normalized to the control group. ANOVA was used to compare between group means. Each scatter dot indicates mean ± S.E.. Between group differences are significant at $p < 0.0001$, denoted by ***; day 3 through day 5 were significantly different at $p = 0.05$, denoted by *

Furthermore, SNAT has favorable physicochemical properties, including small near-atomic size, positive surface charge, aqueous solubility, and stability for over 3 years at room temperature and thus does not require cold storage chain during transportation and storage. The lack of cold storage infrastructure has been identified as one of the reasons impeding vaccine delivery across the low-income nations around the globe, widening the inequality to vaccine access [34]. In this regard, novel inhalation antiviral therapeutics, such as SNAT, that do not require refrigeration or cold storage chain would be ideal to transport from industry in the form of inhaler to patients at home or the clinical setting without the need for refrigeration.

Recently, a trivalent nanobody called ALX-0171 was developed and delivered via a nebulizer in patients infected with respiratory syncytial virus (RSV) in a phase 2b clinical trial [35]. Although RSV clearance was noted, treatment after the infection was established in lower respiratory pathway did not provide clinical benefits to patients, suggesting for treatment intervention during the earlier

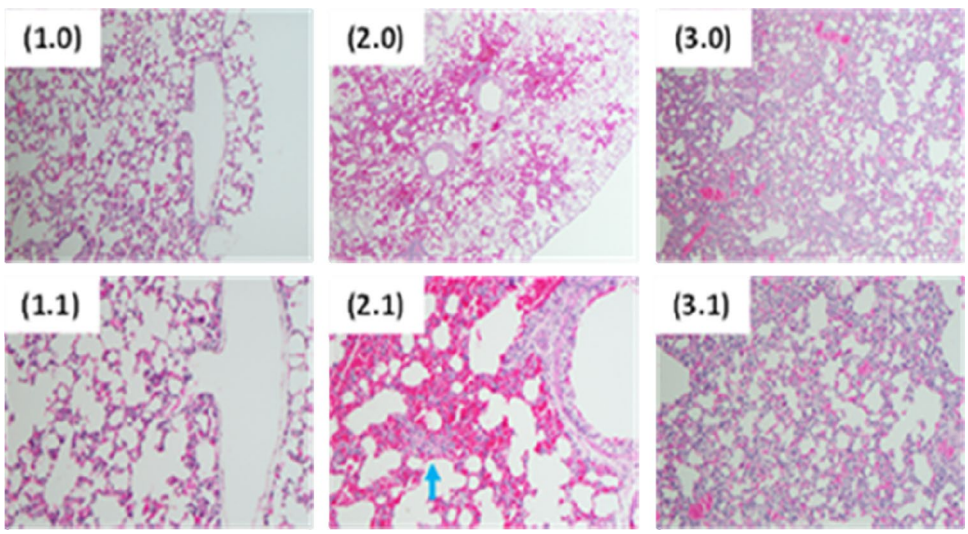

Fig. 6 SNAT improves lung health in SARS-CoV-2-infected hamster. Hematoxylin and eosin (H&E) staining of the lungs of hamsters challenged with SARS-CoV-2 with or without SNAT treatment at 3 dPI. Panels 1.0 and 1.1; 2.0 and 2.1; and 3.0 and 3.1 denote lungs from uninfected control, SARS-CoV-2 infected, and SARS-CoV-2 infected and treated with SNAT at 2.0X and 20X magnifications, respectively. Blue arrow denotes focal hyaline membrane formation

stage of infection [35]. In our study, early administrations (2 h and 48 h post infection with SARS-CoV-2) of inhaled SNAT conferred significant protection from the weight loss (Fig. 5) and showed improved lung health (Fig. 6; panels 3.0 and 3.1), unlike in hamsters infected with SARS-CoV-2 that showed patchy oedema, hemorrhage and vascular congestion, subtle mononuclear infiltration, and focal hyaline membrane formation in lungs (Fig. 6; panels 2.0 and 2.1).

The latest in the development of antiviral therapy against COVID-19 is Merck and Ridgeback's experimental oral pill called Molnupiravir (MK-4482/EIDD-2801), a potent ribonucleoside analog that inhibits the replication of SARS-CoV-2. Although initially touted to have 50% protection [36], recent analyses suggest that the drug could only reduce the rate of hospitalization or death by 3% (absolute risk reduction) or 30% (relative risk reduction) among SARS-CoV-2-infected patients ($n = 1{,}433$) [37]. In addition, FDA has indicated that Molnupiravir may not be safe to pregnant women owing to its potential for "lethal mutagenesis" and/or off-target effects [38]. Considering these limitations and with the global rise of new variants that are potentially more infectious, and because current therapeutics require intravenous or oral delivery and/or access to COVID healthcare facilities, improving drug access to those underprivileged would require engineering future antiviral therapeutics that are easy to deliver at home without the need for a health care facility, which can be achieved using a ready-to-use inhaler or nebulizer akin to that used for SNAT.

Conclusions

Despite concerted global efforts in the fight against COVID-19, the availability of only a few antiviral therapeutics warrants more effective treatment options that can provide significant relief not only to COVID-19 patients and their families but also to the healthcare workers and hospitals that have suffered significant brunt of the pandemic [39]. In this proof-of-concept study, we show that SNAT (Tx–[NH_2-AgNPs]) can effectively inhibit SARS-CoV-2 replication in golden Syrian hamster, protect them from body weight loss and improve lung health, and is non-toxic/safer to human skin and lung cells. These promising pilot preclinical results suggest SNAT as a novel, easy-to-deliver, potent yet biocompatible antiviral drug lead against SARS-CoV-2 infections and may find applications as a platform technology against other respiratory viruses of epidemic and pandemic potential.

Supplementary information The online version contains supplementary material available at https://doi.org/10.1007/s13346-022-01166-x.

Acknowledgements We thank the veterinarians, technicians, and staff in the ECU Department of Comparative Medicine for their support with animal housing and care.

Author contribution LRP and SMA conceived and designed the study. LRP rationally designed, synthesized, purified, characterized, and patented the SNAT. LRP and SMA contributed equally to the analysis of data and wrote the manuscript. SMA and LRP co-led the team and performed the hamster studies including the LDH and MDA assays. FW actively participated in hamster and in vitro studies. PPC provided input to the study design and manuscript. DO contributed to the design of the nose-only exposure system and supervised the animal housing and care in the BSL-3 facility. GM preformed the histopathology study. All co-authors read and approved the manuscript.

Funding This work was partially supported by funds from East Carolina University (ECU grant #111101) and ECU Office of Commercialization and Licensing (National Science Foundation I-Corps) to L.R.P., and North Carolina Biotechnology Center's Flash Grant (grant #2021-FLG-3812) to L.R.P. and S.M.A.

Availability of data and materials All data that support the findings of this study are presented in the main text.

Declarations

Ethics approval and consent to participate Our Animal Use Protocol entitled, "Effect of SNAT on SARS-CoV-2 infection of hamsters" (AUP #K177) was reviewed and approved by ECU Institution's Animal Care and Use Committee (IACUC) (approval date: 11/12/2020). The use of biohazardous agent (SARS-CoV-2) was approved by ECU Office of Prospective Health/Biological Safety (registration #20–01; Title: Host response to COVID-19 infection in Eastern North Carolina). There were no human participants involved in this research.

Consent for publication NA.

Competing interests All the patents' rights (US Patent No. 63/042,070, and US Patent No. PCT/US2021/014343) are owned by East Carolina University and L.R.P. is the sole inventor.

References

1. Feng W, Zong W, Wang F, Ju S. Severe acute respiratory syndrome coronavirus 2 (SARS-CoV-2): a review. Mol Cancer. 2020;19(1):100.
2. Jamal M, Bangash HI, Habiba M, Lei Y, Xie T, Sun J, Wei Z, Hong Z, Shao L, Zhang Q. Immune dysregulation and system pathology in COVID-19. Virulence. 2021;12(1):918–36.
3. World Health Organization. Severe acute respiratory syndrome (SARS). WHO 2022. Available at: https://www.who.int/health-topics/severe-acute-respiratory-syndrome#tab=tab_2. Accessed 20 Dec 2021.
4. Yong SJ. Long COVID or post-COVID-19 syndrome: putative pathophysiology, risk factors, and treatments. Infect Dis (Lond). 2021;1–18.
5. Krumm ZA, Lloyd GM, Francis CP, Nasif LH, Mitchell DA, Golde TE, Giasson BI, Xia Y. Precision therapeutic targets for COVID-19. Virol J. 2021;18(1):66.
6. Twomey JD, Luo S, Dean AQ, Bozza WP, Nalli A, Zhang B. COVID-19 update: the race to therapeutic development. Drug Resist Updat. 2020;53:100733.

7. Donalisio M, Leone F, Civra A, Spagnolo R, Ozer O, Lembo D, et al. Acyclovir-loaded chitosan nanospheres from nano-emulsion templating for the topical treatment of herpesviruses infections. Pharmaceutics. 2018;10:46.
8. Dormont F, Brusini R, Cailleau C, Reynaud F, Peramo A, Gendron A, et al. Squalene-based multidrug nanoparticles for improved mitigation of uncontrolled inflammation. Sci Adv. 2020:eaaz5466.
9. Novavax Inc. Novavax awarded funding from CEPI for COVID-19 vaccine development. IR Site. Available from: https://ir.novavax.com/news-releases/news-release-details/novavax-awarded-funding-cepi-covid-19-vaccine-development. Accessed 22 Dec 2021.
10. World Nano Foundation. COVID-19 report & analysis. Available from: https://www.worldnanofoundation.com/covid-19-report-analysis. Accessed 25 Mar 2022.
11. Chakravarty M, Vora A. Nanotechnology-based antiviral therapeutics. Drug Deliv Transl Res. 2021;11(3):748–87. https://doi.org/10.1007/s13346-020-00818-0.
12. Pek Z, Cabanilla MG, Ahmed S. Treatment refractory Stenotrophomonas maltophilia bacteraemia and pneumonia in a COVID-19-positive patient. BMJ Case Rep. 2021;14(6).
13. Nagesh CP. The "black fungus" through a gray lens: imaging COVID-19-associated mucormycosis. Indian J Ophthalmol. 2021;69(7):1648–9.
14. Wang B. Adjusting extracellular pH to prevent entry of SARS-CoV-2 into human cells. Genome. 2021;64(6):595–8.
15. Imai M, Iwatsuki-Horimoto K, Hatta M, Loeber S, Halfmann PJ, et al. Syrian hamsters as a small animal model for SARS-CoV-2 infection and countermeasure development. Proc Natl Acad Sci USA. 2020;117(28):16587–95.
16. Sia SF, Yan LM, Chin AWH, Fung K, Choy KT, et al. Pathogenesis and transmission of SARS-CoV-2 in golden hamsters. Nature. 2020;583(7818):834–8.
17. Brocato RL, Principe LM, Kim RK, Zeng X, Williams JA, et al. Disruption of adaptive immunity enhances disease in SARS-CoV-2-infected Syrian hamsters. J Virol. 2020;94(22).
18. Dyson OF, Walker LR, Whitehouse A, Cook PP, Akula SM. Resveratrol inhibits KSHV reactivation by lowering the levels of cellular EGR-1. PLoS One. 2012;7(3):e33364.
19. Akula SM, Bolin P, Cook pp. Cellular miR-150-5p may have a crucial role to play in the biology of SARS-CoV-2 infection by regulating nsp10 gene. RNA Biol. 2022;19(1):1–11.
20. Walker LR, Hussein HA, Akula SM. Subcellular fractionation method to study endosomal trafficking of Kaposi's sarcoma-associated herpesvirus. Cell Biosci. 2016;6:1.
21. Hussein HAM, Akula SM. miRNA-36 inhibits KSHV, EBV, HSV-2 infection of cells via stifling expression of interferon induced transmembrane protein 1 (IFITM1). Sci Rep. 2017;7(1):17972.
22. Karpenko IL, Valuev-Elliston VT, Ivanova ON, Smirnova OA, Ivanov AV. Peroxiredoxins-the underrated actors during virus-induced oxidative stress. Antioxidants (Basel). 2021;10(6).
23. Luo M, Wu L, Zhang K, Wang H, Zhang T, et al. miR-137 regulates ferroptosis by targeting glutamine transporter SLC1A5 in melanoma. Cell Death Differ. 2018;25(8):1457–72.
24. Reddy PV, Gandhi N, Samikkannu T, Saiyed Z, Agudelo M, et al. HIV-1 gp120 induces antioxidant response element-mediated expression in primary astrocytes: role in HIV associated neurocognitive disorder. Neurochem Int. 2012;61(5):807–14.
25. Paracha UZ, Fatima K, Alqahtani M, Chaudhary A, Abuzenadah A, et al. Oxidative stress and hepatitis C virus. Virol J. 2013;10:251.
26. Lee YH, Lai CL, Hsieh SH, Shieh CC, Huang LM, et al. Influenza A virus induction of oxidative stress and MMP-9 is associated with severe lung pathology in a mouse model. Virus Res. 2013;178(2):411–22.
27. Zhang Z, Rong L, Li YP. Flaviviridae viruses and oxidative stress: implications for viral pathogenesis. Oxid Med Cell Longev. 2019;1409582.
28. Wang C, Kang K, Lan X, Fei D, Wang Q, Li X, Chong Y, Gao Y, Wang H, Li X, Zhao M, Yu K. Cytokine levels in sputum, not serum, may be more helpful for indicating the damage in the lung and the prognosis of severe COVID-19 - a case series. J Infect. 2021;83(5):e6–9.
29. Cagno V, Andreozzi P, D'Alicarnasso M, et al. Broad-spectrum non-toxic antiviral nanoparticles with a virucidal inhibition mechanism. Nat Mater. 2018;17(2):195–203. https://doi.org/10.1038/nmat5053.
30. Medhi R, Srinoi P, Ngo N, Tran H-V, Lee R. Nanoparticle-based strategies to combat COVID-19. ACS Appl Nano Mater. 2020;3(9):8557–80.
31. Eggleton JJ, Nagalli S. Highly active antiretroviral therapy (HAART). StatPearls, StatPearls Publishing Copyright© 2022, StatPearls Publishing LLC, Treasure Island (FL), 2022.
32. Leyssen P, De Clercq E, Neyts J. Molecular strategies to inhibit the replication of RNA viruses. Antiviral Res. 2008;78(1):9–25.
33. Cao J, Liu Y, Zhou M, Dong S, Hou Y, et al. Screening of botanical drugs against SARS-CoV-2 entry reveals novel therapeutic agents to treat COVID-19. Viruses. 2022;14(2).
34. Hinnant L, Mdenick S. Vaccine storage issues could leave 3B people without access. AP News. 2020. https://apnews.com/article/virus-outbreak-pandemics-immunizations-epidemics-united-nations-fc4c536d62c5ef25152884adb1c14168. Accessed 20 Dec 2021.
35. Cunningham S, Piedra PA, Martinon-Torres F, Szymanski H, Brackeva B, et al. Nebulised ALX-0171 for respiratory syncytial virus lower respiratory tract infection in hospitalized children: a double-blind, randomised, placebo-controlled, phase 2b trial. Lancet Respir Med. 2021;9:21–32.
36. Merck and Ridgeback's investigational oral antiviral molnupiravir reduced the risk of hospitalization or death by approximately 50 percent compared to placebo for patients with mild or moderate COVID-19 in positive interim analysis of phase 3 study. 2021. Available at: https://www.merck.com/news/merck-and-ridgebacks-investigational-oral-antiviral-molnupiravir-reduced-the-risk-of-hospitalization-or-death-by-approximately-50-percent-compared-to-placebo-for-patients-with-mild-or-moderat/. Accessed 25 Mar 2022.
37. Merck and Ridgeback biotherapeutics provide update on results from MOVe-OUT study of molnupiravir, an investigational oral antiviral medicine, in at risk adults with mild-to-moderate COVID-19. 2021. Available at: https://www.merck.com/news/merck-and-ridgeback-biotherapeutics-provide-update-on-results-from-move-out-study-of-molnupiravir-an-investigational-oral-antiviral-medicine-in-at-risk-adults-with-mild-to-moderate-covid-19/. Accessed 25 Mar 2022.
38. Ledford H. COVID antiviral pills: what scientists still want to know. Nature. 2021;599:358–9.
39. Kaushik D. Medical burnout: breaking bad. 2021. Available at: https://www.aamc.org/news-insights/medical-burnout-breaking-bad. Accessed 20 Dec 2021.